PREPARATION, DEPOSITION OF $Cu(In_{1-X}Ga_X)Se_2$ NANOPOWDER THIN FILMS BY NON-VACUUM PROCESSES AND ITS CHARACTERIZATION

S. Velumani, B. J. Babu, B. Vidhya, P. Reyes, A. Angeles and R. Asomoza
Department of Electrical Engineering-SEES, CINVESTAV-IPN, Zacatenco, Mexico D.F., C.P. 07360, Mexico

ABSTRACT

Non-vacuum techniques for the preparation of $Cu(In_{1-x}Ga_x)Se_2$(CIGS) nanoparticle films is reported. CIGS nanoparticles were prepared by mechano-chemical process followed by screen printing and air-brush spray with suitable solvent. Elemental Cu/In/Ga/Se sources were ball milled with different milling times and rates to optimize the conditions to obtain chalcopyrite composition. Under the optimized conditions, gallium composition was varied from x=0.1-0.5 to obtain single phase CIGS nanoparticle. XRD revealed the polycrystalline and chalcopyrite structure with an intense (112) orientation. Grain sizes varied from 8 to 20 nm and 2θ values of (112) plane shifted towards higher angle confirming the gallium incorporation into indium sites. TEM/HRTEM analyses revealed the presence of nanocrystalline particles and SAED pattern correspond to peaks found from XRD, d-spacing values were found to be 1.06, 3.33, 2.03 and 0.906Å corresponding to the diffraction patterns and simulated patterns are matched with HRTEM planes. Raman spectra showed intense peak at 168–172cm^{-1}, corresponding to chalcopyrite structure. Viscosities, ratio of solvents versus nanopowders were optimized, in order to make films using screen printing and air brush spray. Screen printed films were annealed in N_2 atmosphere from 300-400^0 C and no significant growth in particle size observed. Loss of gallium was estimated from EDAX and peak value (2θ) of the plane (112) shifted towards left. Hall studies yielded the carrier concentration of 10^{14} cm^{-3} and di-electric constant decreased with increase in frequency and increased with temperature (298-398K). Photoconduction studies revealed an increase in current with light intensity/thickness. Glass/ITO/CdZnS/CIGS/Ag device was made and characterized by I-V yielding open circuit voltage 300 mV, short circuit current density, 126.7 μA cm^{-2} and fill factor close to 0.25.

INTRODUCTION

Semiconductors AI–BII–CVI_2 compounds and solid solutions based on them are unique objects for the study of the fundamental properties of chalcopyrite semiconductors. A special place among them is occupied by quaternary system containing Cu, In, Ga and Se which is proven for photovoltaic applications, possessing high absorption coefficient (10^4-10^5 cm^{-1}), direct band gap (1.02-1.7eV) and stability against photo degradation [1]. The photoelectric conversion efficiency of CIGS cell has reached 20.1% in lab scale and exceeded 13% for large area modules [2]. A $CuInSe_2$-based solar cell performance has been improved by the addition of Ga to form CIGS absorber layers [3]. The optical band gap of CIS is 1.02 eV which is less than the optimum value required for PV cells. However, the band gap of CIS can be varied from 1.02 eV to 1.7 eV by selective incorporation of gallium [1]. Commonly used methods for the synthesis of CIGS nanoparticles include solvothermal technique, low temperature colloidal synthesis [4,5], etc. Among them, solvothermal technique is time consuming, for example a reaction temperature of 280 ◦C for 36 h and then cooling to room temperature [4]. Low temperature colloidal synthesis uses Na_2Se as one of the starting materials, which is highly toxic [5]. CIGS thin films are usually deposited by either multi-source thermal evaporation of the individual components or sputtering [6] and subsequent co-deposition or reactive annealing of precursor Cu-In-Ga films in a selenium atmosphere These processes are usually long, contain a number of deposition and annealing steps which are expensive. Non-vacuum techniques [7,8] are used to bring down the cost and scalability to larger area. Therefore, mechanical alloying of blended elemental powders and subsequent film deposition (spray pyrolysis, screen printing, inket printing, etc) of the milled powders was considered as a simple and inexpensive alternate process to produce the CIGS alloy. In this work we realized preparation of CIGS nanoparticles with various Ga composition and their thin films prepared by non vacuum process such as screen printing and air brush spray. We report optimum conditions for preparing single phase CIGS nanoparticles, screen printed films and air brush sprayed films. An approach to preparation of CIGS based superstrate devices was undertaken.

EXPERIMENTAL

$Cu(In_{1-x}Ga_x)Se_2$ nanopowders were synthesized by mechanical alloying using Retsch PM400 planetary ball mill, mixing high purity (99.99%, Sigma-Aldrich) powder precursors of copper, indium, granulated gallium and selenium. Precursors and tungsten carbide balls were sealed in a tungsten carbide vial in argon atmosphere using a glove box and then ball milled, leading to the formation of CIGS nanoparticles. Initially for a fixed milling time (2h) powders were prepared with three different rotational speeds 300, 350 and 400 rpm. Then rotational speed was fixed at 400 rpm and milling time was varied from 45 min to 4 hrs at 30 minutes interval. Finally, after optimizing the speed(400 rpm) and milling time (2hrs) from above two steps, gallium concentration in $Cu(In_{1-x}Ga_x)Se_2$ is varied (x=0.1, 0.2, 0.3, 0.4 and 0.5). CIGS nanoparticle powder prepared by ball milling is mixed with an organic binder ethyl cellulose followed by the addition of ethylene glycol and ethyl alcohol, which was mixed thoroughly until a semi paste like ink is obtained. This precursor was used

for screen printing on glass substrates at room temperature and spray-deposition using a commercially available airbrush kit (Iwata Kustom TH) with pressurized nitrogen as the carrier gas at 100^0C. Films grown using screen printing are subjected to rapid and slow annealing at five different temperatures from 300 to 400^0C in nitrogen ambient. Commercially available ITO substrates were used as the top contact material onto which CdZnS thin films were deposited by Microwave assisted Chemical bath deposition (MW-CBD) followed by screen printing of CIGS nanoparticle powders and sintering at 400^oC. Silver contacts were deposited on the structure Glass/ITO/CdZnS/CIGS for electrical measurements. The performance of fabricated PV cell have been studied by illuminating it using a ELH lamp[120 V, OSRAM] and the light intensity has been measured using a standard cell (123mV). X-ray diffraction were performed at room temperature with a CuKα radiation (λ=1.54051Å) by XPERT-PRO system with a scan step size of 0.05. Bruker EDAX sytem attached to Carls Zeiss-AURIGA FESEM has been used to determine composition of CIGS powder. Raman measurements were carried out at room temperature using a Olympus BX41 Horiba Jobin Yvon micro-Raman system with laser wavelength of 632nm with a power of 20 mW. HRTEM images were obtained with a FEI Tecnai F30 transmission electron microscope operating with beam energy of 300KV.

RESULTS AND DISCUSSION

Preparation of CIGS nanopowders

Optimum conditions for preparing mechanochemically single phase CIGS nanoparticles are reported. Considering the fact that, milling speed plays a vital role in defining the final composition and size of nanoparticles [9] and that the formation of single phase CIGS is not obtained at low rpm (<300 rpm), this work is focused on milling speed equal to or more than 300 rpm. X-ray diffraction pattern of $CuIn_{0.7}Ga_{0.3}Se_2$ nanopowders at fixed milling time prepared for 300, 350 and 400 rpm (see Fig.1) shows pure phase CIGS powder is obtained with a milling speed of 400 rpm, indicating that a stronger impact force (higher energy input) is acting during the formation of the nanopowder. From XRD as a function of milling time (see Fig.2) at 400 rpm, it is observed that $CuIn_{0.7}Ga_{0.3}Se_2$ phase formed after 2 hours of milling and for more duration, no change in phase is detected. At this 2 hrs, the process achieved a steady state between fracturing and cold welding of powder particles. Hence 2 hrs milling time at 400 rpm will be optimum parameters for preparing single phase CIGS nanoparticles. Samples prepared at this optimum parameters with different Ga concentrations (from x=0.1 to x=0.5) presented (see Fig. 3) a decrease in FWHM (1.05° to 0.85° from x=0.1 to 0.5 for (112) plane) of peaks with the increase in Ga content, consequently peaks in XRD shifting towards right were observed due to the decrease in lattice parameters 'a' and 'c' with increasing gallium concentration [10]. HRTEM images as well as Fourier transformation in reciprocal space provide

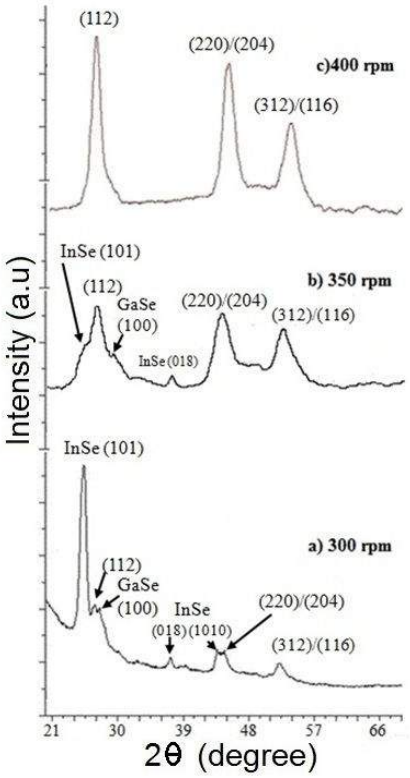

Figure 1 X-ray Diffraction pattern of ball milled $CuIn_{0.3}Ga_{0.7}Se_2$ nanopowder.

a proper way to identify the structure of CIGS nanocrystals. From HRTEM analyses of $CuIn_{0.7}Ga_{0.3}Se_2$ sample, in the inset of Fig. 4a, Fast Fourier Transform (FFT) denotes a polycrystalline material, which must be composed of nanocrystals. The d-spacing corresponding to (1 1 2), (2 2 0)/(2 0 4), (3 1 2)/(4 1 7) and (6 2 0)/(6 0 4) diffraction peaks of CIGS has been observed, which again confirms the chalcopyrite structure of the samples. In order to confirm the best fit among these planes, we have simulated the crystal planes of CIGS chalcopyrite structure using SimulaTEM/DFT calculations and matched it with the HRTEM pattern (see Fig. 4b). Raman studies showed (see Fig. 5a) A1 phonon mode, which is the strongest mode generally observed for chalcopyrite compounds [11], shifting to the right in the frequency range 167–170 cm^{-1} indicating an increase in Ga content [12]. The A1 mode is broadened for Cu-poor absorbers due to defects [13]. A linear dependence of the frequency of the A1-mode (see Fig. 5b) on the powder composition has been found. This is in agreement with linear dependence of frequency of A1 mode with increase in gallium content as reported by Papadimitriou, et al (2005) [14].

Characterization of screen printed and air brush sprayed CIGS thin films

An initial attempt to find an economic CIGS deposition system is realized. In this work a non-vacuum particulate

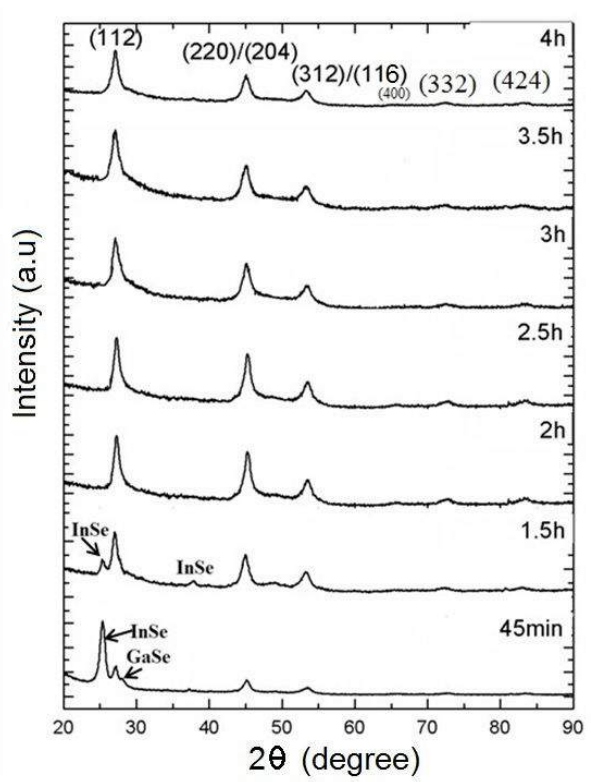

Figure 2 XRD pattern of $CuIn_{0.3}Ga_{0.7}Se_2$ as a function of milling time.

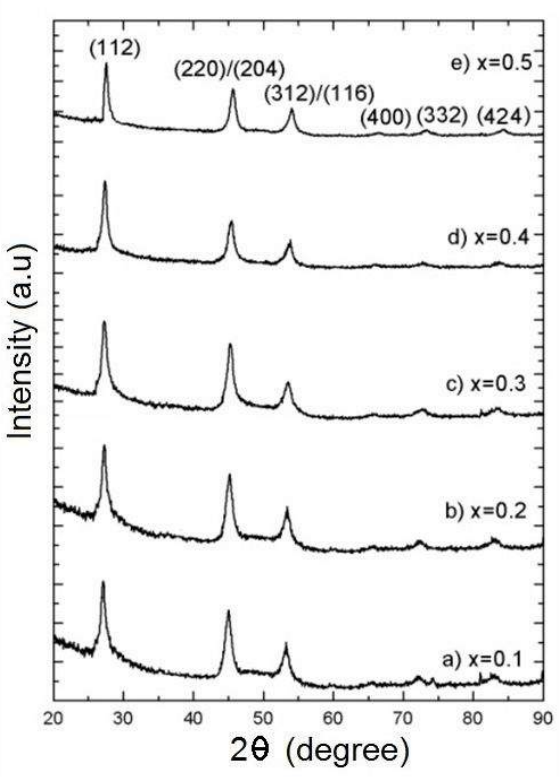

Figure 3 X-ray diffraction patterns for different Ga concentrations.

ink based technique is used for depositing CIGS as a film in a two-step approach, where a precursor is deposited at low temperature and then followed by annealing treatment. For the screen printed films (see Fig. 6) annealed in nitrogen, there were no traces of secondary phases. There was no significant grain growth in the temperature range from 100 to 400°C and hence maintaining the nanoparticle size. Peak shift to lower angles in XRD patterns without remarkable growth of particles has been noticed, confirming the negligible effect of strain in these films. Therefore XRD peak shift of $CuIn_xGa_{1-x}Se_2$ is considered to be related to Ga contents in film, where, as Ga content increases, lattice constant decreases and subsequently the diffraction angle increases [15]. This was further confirmed by EDAX analysis where it was observed that higher the heat treatment temperature was, lower were the Ga content in films as given in Table 1. XRD patterns (see Fig. 7) of airbrush spray deposited films annealed at 250 °C in room atmosphere, are found to exhibit (112), (220)/(204) and (312)/(116) planes corresponding to chalcopyrite structure of $CuIn_{1-x}Ga_xSe_2$. Grain size almost remained the same compared with powder precursors. As in the screen printed samples, effect of strain is negligible, therefore peak shifting to higher diffraction angles (see Fig. 7) for films with x=0.1 to 0.5 is related to lattice constants decrease with increasing Ga incorporation to the structure.

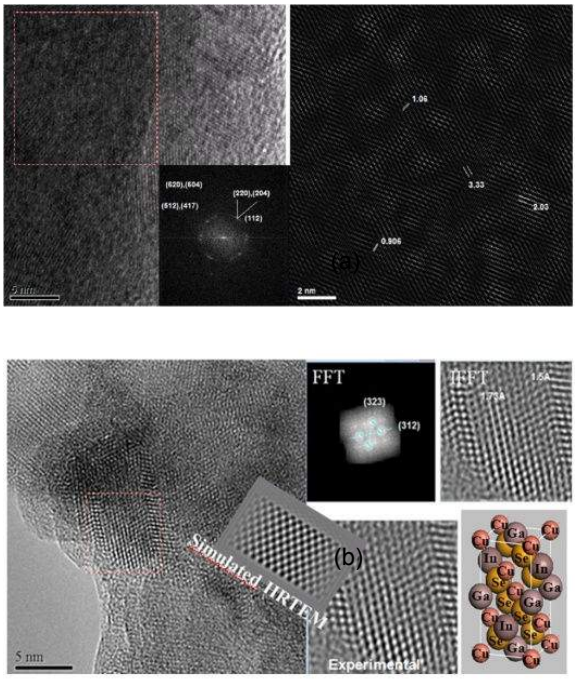

Figure 4 HRTEM analyses, (a) determination of structure with help of interplanar distance measurement and (b) Simulated patterns are matched with HRTEM planes.

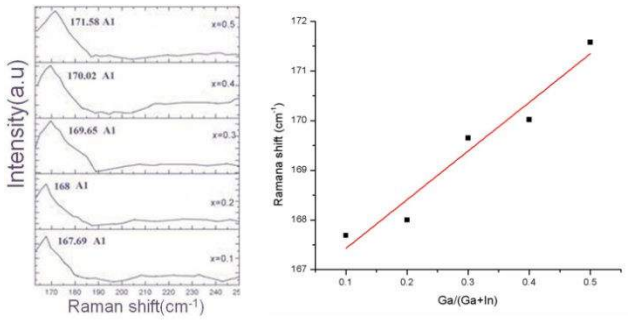

(a) (b)

Figure 5 Raman spectra of CIGS nanopowders (a) different Ga concentration and (b) A1 mode linear dependence with Ga.

For screen printed CIGS films, the variation of dielectric constant with frequency at different temperatures (see Fig.8) shows that the dielectric constant decreases with the frequency at all temperatures. Photocurrent (see Fig. 9) is found to increase with an increase in film thickness and light intensity. As thickness of film increases the crystalline nature increases and this helps in improvement of photocurrent. The increase in photocurrent is attributed to an increase in the majority carrier concentration and/or an increase in impurity centers acting as traps for minority carriers [16]. The increase in photocurrent with light intensity may be mainly due to the reduction in barrier height (E_b) rather than the increase in majority carriers. The decrease in E_b will result in the increase in minority carriers, which flow down the barriers to neutralize the trap states at the grain boundaries.

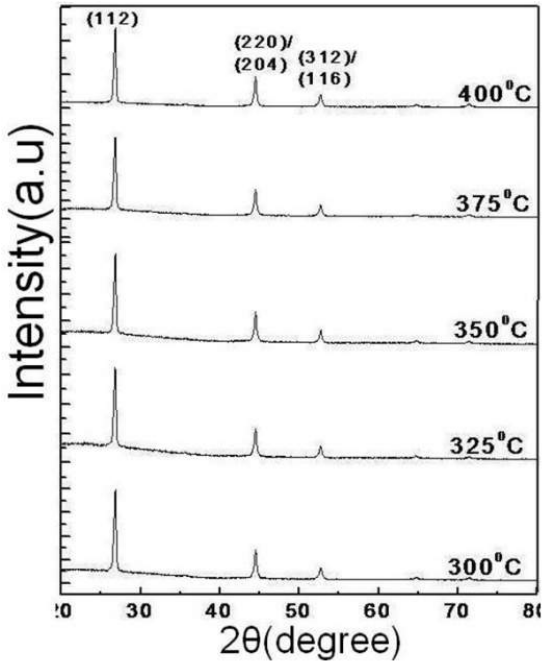

Figure 6 XRD pattern of screen printed $CuIn_{0.75}Ga_{0.25}Se_2$ films.

Annealing Temperature°C	Cu at%	In at%	Ga at%	Se at%
300	25.71	21.06	4.71	48.52
325	25.72	20.73	4.81	48.74
350	25.86	20.21	5.12	48.81
375	25.52	20.08	4.15	50.25
400	25.81	19.29	4.23	50.67

Table 1. Composition of screen printed films

Characterization of ITO/*n*-CdZnS/*p*-CIGS superstrate device structure.

Chemicals used for CdZnS consist on aqueous solutions of 5.8x10-3 mol/l 3CdSO4.5H2O, 0.037 mol/l NH3SO4, 0.065 mol/l H2NCSNH2, 1.738x10-3 mol/l ZnSO4.7H2O and 1.5 mol/l NH3; chemical bath temperature was maintained in the range between 90oC to 95oC, a cyclic microwave irradiation is applied to bath solution and the deposition time varied from 60 s to 180 s [17]. An attempt has been made to fabricate ITO/*n*-CdZnS/*p*-$CuIn_{0.75}Ga_{0.25}Se_2$ (nanopowders) PV cells by CdZnS MW-CBD and CIGS screen printing process. Current-voltage characteristics of fabricated PV cell (see Fig.10) yielded open circuit voltage 300 mV, short circuit current density 126.7 μA cm^{-2} and fill factor close to 0.25. Conversion efficiencies of the fabricated PV cells are found to be 0.01-0.1%. Low efficiency may be due to the low shunt resistance which may be caused by leakage of current across the semiconductor surface or high value of series resistance due to high resistivity of the absorber layer (KΩ). Finally as the deposition techniques are completely non-vacuum, there is every possibility for the formation of an insulating layer between the two layers, also affecting the efficiency of fabricated PV cells.

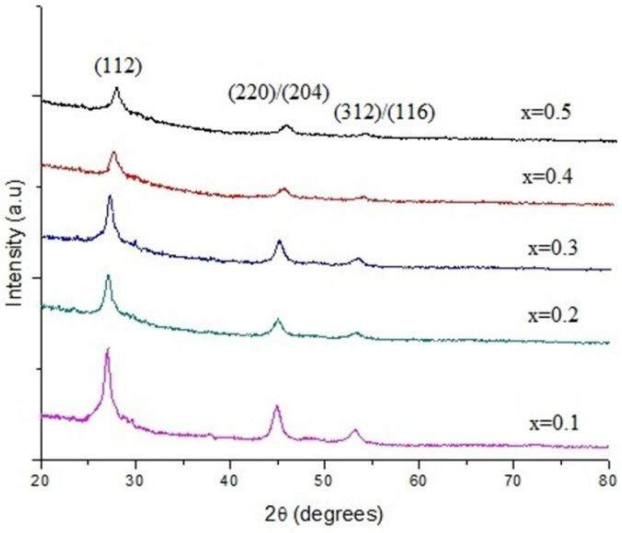

Figure 7 XRD pattern of air brush sprayed CIGS film with different Ga.

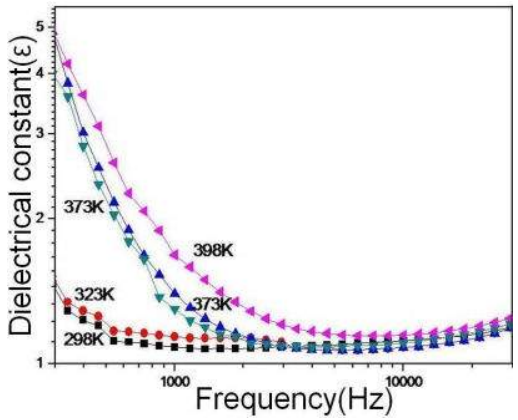

Figure 8 Dielectric constant vs frequency.

This study explains the formation of CIGS nanoparticles and its film formation using low cost non-vacuum techniques. However, further compositional studies on airbrush deposited films are required in order to know the effects of annealing in the film stoichiometry and in the entirely PV device.

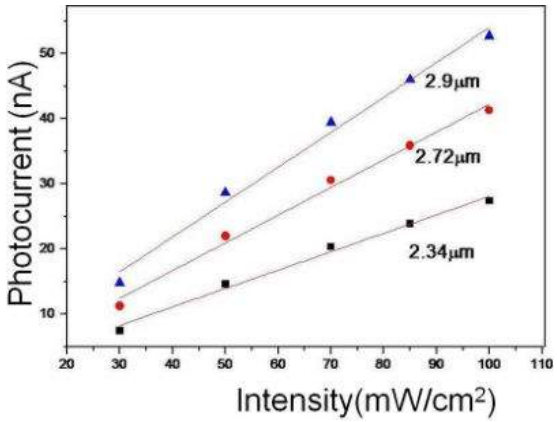

Figure 9 Photoconduction studies on screen printed $CuIn_{0.75}Ga_{0.25}Se_2$ thin films.

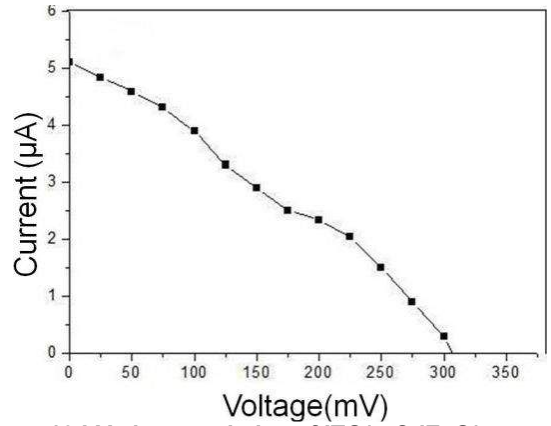

Figure 10 I-V characteristics of ITO/n-CdZnS/p-$CuIn_{0.75}Ga_{0.25}Se_2$ PV cell.

CONCLUSIONS

Effect of *x* (0.1-0.5) on the structural properties of ball milled $Cu(In_{1-x}Ga_x)Se_2$ nanoparticles showed a decrease in lattice constants and increase in grain size with the increase in *x*, this is due to the small ionic size of Ga (0.62 Å) compared to In (0.81 Å) causing shrinkage of the lattice as they substitute indium sites in the cell. CIGS nanoparticles were prepared for different milling time and speed. EDAX results revealed the loss of Se with the increase in milling time due to low volatilization temperature of Se. It has been concluded that single phase CIGS nanoparticles can be prepared by ball milling for 2 hours at 400rpm. XRD results confirm deposition of CIGS using screen printing and airbrush spray technique. XRD of screen printed films show a shift in peak towards lower angle with the increase in temperature of heat treatment. This is because of thermodynamically unstable nano sized particles [9]. Photoconduction studies showed the increase in current with the increase in light intensity, supporting the use of this material for PV application. ITO/CdZnS/CIGS solar cells were fabricated and obtained low efficiencies (< 0.1%) due to too small CIGS grains, porous structures of the absorber layer, laboratory conditions etc. However, these results demonstrate the possibility of a low cost non-vacuum process for CIGS thin film solar cells.

REFERENCES

[1] *Y.H.A Wang, C. Pan, N. Bao and A. Gupta,"* Synthesis of ternary and quaternary $CuIn_xGa_{1-x}Se_2$ semiconductor nanocrystals*",* Solid State Sciences 11, 2009, pp. 1961–1964.

[2] Z. Ning, Z. Da-Ming and Z. Gong, "An investigation on preparation of CIGS targets by sintering process", Materials Science and Engineering B 166, 2010, pp. 34–40.

[3] C. Huang, "Effects of Ga content on Cu(In,Ga)Se2 solar cells studied by numerical modeling", Journal of Physics and Chemestry of Solids 69, 2008, pp. 330-334.

[4] Y. Chun, K. Kim and K. Yoon," Synthesis of CuInGaSe2 nanoparticles by solvothermal route", Thin Solid Films 480–481, 2005, pp. 46–49.

[5] S. Ahn, K. Kim, Y. Chun and K. Yoon," Nucleation and growth of $Cu(In,Ga)Se_2$ nanoparticles in low temperature colloidal process", Thin Solid Films 515, 2007, pp.4036–4040.

[6] F. Adurodija, J. Song, S. Kim, S. Kwon, S. Kim, K. Yoon and B. Ah, "Growth of $CuInSe_2$ thin films by high vapour Se treatment of co-sputtered Cu-In alloy in a graphite container", Thin Solid Films 338/1–2, 1999, pp. 13-19.

[7] C. Eberspacher, C. Fredric, K. Pauls and J. Serra**,** "Thin-film CIS alloy PV materials fabricated using non-vacuum, particles-based technique", Thin Solid Films 387/1–2, 2001, pp. 18-22.

[8] K. Kapur, A. Bansal, P. Le and O. Asensio**, "**Non-vacuum processing of $CuIn_{1-x}Ga_xSe_2$ solar cells on rigid

and flexible substrates using nanoparticle precursor inks**",** Thin Solid Films 431–432, 2003, pp. 53-57.
[9] Kuhrt C, Schropf H, Schultz L, Arzt E. In: deBarbadillo JJ, et al., editors. "Mechanical alloying for structural applications: Proceedings of the 2nd International Conference on Structural Applications of mechanical Alloying 2", International Conference on Structural Applications of Mechanical alloying, 1993, pp. 269-73.
[10] W. Witte, R. Kniese, M. Powalla. "Raman investigations of Cu(In,Ga)Se2 thin films with various copper contents", Thin Solid Films 517, 2008, pp. 867–869.
[11] S. Roy, P. Guhaa, S.N. Kundu, H. Hanzawa, S. Chaudhuri, A.K. Pal. "Characterization of Cu(In,Ga)Se2 films by Raman scattering", Materials Chemistry and Physics 73, 2002, pp. 24–30.
[12] D. Papadimitriou, N. Esser and C. Xue, "Structural properties of chalcopyrite thin films studied by Raman spectroscopy", Phys. Stat. Sol. (b) 242, 2005, pp. 2633–2643.
[13] T. Chen, J. M. Hampkian and N. N. Thadhani. "Synthesis and characterization of mechanically alloyed and shock-consolidated nanocrystalline NiAl intermetallic", Acta mater. 47, 1999, pp. 2567-2579.
[14] D. Papadimitriou, N. Esser and C. Xue. "Structural properties of chalcopyrite thin films studied by Raman spectroscopy" Phys. Stat. Sol. (b) 242, 2005, pp. 2633–2643.
[15] J. Olejnicek, C.A. Kamler, A. Mirasano, A.L. Martinez-Skinner, M.A. Ingersoll, C. L. Exstrom, S. A. Darveau, J. L. Huguenin-Love, M. Diaz, N. J. Ianno and R.J.Soukup. ""A Non-Vacuum Process for Preparing Nanocrystalline CuIn1-xGaxSe2 Materials Involving an open-Air Solvothermal Reaction", Solar Energy Materials & Solar Cells 94, 2009, pp. 8-11.
[16] B.Vidhya**,** S.Velumani and R.Asomoza, "Effect of milling time and heat treatment on the composition of $CuIn_{0.75}Ga_{0.25}Se_2$ nanoparticle precursors and films", *Jounal of nanoparticle Research*, 2011 (Article in press).
[17] B. Vidhya and S. Velumani, " Effect of Thickness on the Structural, Optical and electrical Properties of MW-CBD CdZnS Thin Films", Electrical Engineering, Computing Science and Automatic Control,CCE,2009 6th International Conference on, 2010, pp.1-5.